

Spin and orbital hybridization at specifically nested Fermi surfaces in URu₂Si₂

P. M. Oppeneer,¹ S. Elgazzar,² J. Ruzs,¹ Q. Feng,¹ T. Durakiewicz,³ and J. A. Mydosh⁴

¹*Department of Physics and Astronomy, Uppsala University, Box 516, S-75120 Uppsala, Sweden*

²*Physics Department, Johannesburg University, P.O. Box 524, Auckland Park 2006, South Africa*

³*Los Alamos National Laboratory, Condensed Matter and Thermal Physics Group, Los Alamos, NM 87545, USA*

⁴*Kamerlingh Onnes Laboratory, Leiden University, NL-2300 RA Leiden, The Netherlands*

(Dated: October 6, 2011)

The Fermi surface (FS) nesting properties of URu₂Si₂ are analyzed with particular focus on their implication for the mysterious hidden order phase. We show that there exist two Fermi surfaces that exhibit a strong nesting at the antiferromagnetic wavevector, $\mathbf{Q}_0=(0,0,1)$. The corresponding energy dispersions fulfill the relation $\epsilon_1(\mathbf{k})=-\epsilon_2(\mathbf{k}\pm\mathbf{Q}_0)$ at eight FS hotspot lines. The spin-orbital characters of the involved $5f$ states are *distinct* ($j_z=\pm 5/2$ vs. $\pm 3/2$) and hence the degenerate Dirac crossings are symmetry protected in the nonmagnetic normal state. Dynamical symmetry breaking through an Ising-like spin and orbital excitation mode with $\Delta j_z=\pm 1$ induces a hybridization of the two states, causing substantial FS gapping. Concomitant spin and orbital currents in the uranium planes give rise to a rotational symmetry breaking.

PACS numbers: 71.20.-b, 71.27.+a, 74.70.Tx

At temperatures below $T_0=17.5$ K a mysterious hidden order (HO) phase develops¹⁻³ in the heavy-fermion uranium compound URu₂Si₂, the origin of which could not be definitely established despite intensive investigations.⁴ The occurrence of the new, ordered phase below T_0 is clearly witnessed by a sharp, second order phase transition appearing in the thermodynamic and transport quantities.^{1,2,5,6} The appearing new electronic order is not long-range ordered (dipolar) magnetism, although a small pressure of about 0.5 GPa suffices to stabilize long-range antiferromagnetic (AF) order.^{7,8} Recent experimental progress succeeded to reveal particular features of the HO state, thus providing a mosaic of pieces for unraveling the HO.⁹⁻¹⁷ To explain the origin of the HO a large number of sometimes exotic theories have been proposed over a period of more than twenty years¹⁸⁻²⁷ which however could not yet provided a complete understanding (see Ref. 4 for a survey of theories).

A central question concerning the nature of the HO phase is which symmetry is spontaneously broken at the HO transition. A recent torque experiment performed on very small (μm -size) single crystals measured the magnetic susceptibility in the basal a - a plane of the tetragonal unit cell.²⁸ Okazaki *et al.*²⁸ observe rotational symmetry breaking, i.e., the off-diagonal susceptibility χ_{xy} is nonzero in the HO phase, unlike in the normal nonmagnetic phase above T_0 where $\chi_{xy}=0$. To explain the nonzero off-diagonal susceptibility several novel models²⁹⁻³¹ for the HO phase have been put forward recently. The non-vanishing off-diagonal susceptibility has been ascribed to a certain type of quadrupolar order,²⁹ a modulated spin liquid,³⁰ and a spin nematic state.³¹

Apart from breaking of xy -symmetry in the basal plane, it recently became clear that the lattice periodicity along the c^* -axis in the Brillouin zone (BZ) is modified, too, in the HO phase.^{14,15} The body-centered tetragonal (BCT) unit cell of URu₂Si₂ in the normal state becomes doubled in the HO state, and thus becomes simple

tetragonal (ST), consistent with a recent prediction.²³ A complete understanding of the HO state obviously requires an explanation of why both these two symmetry breakings occur, something which has not yet emerged.

Here, we investigate the materials specific characteristics of the nested Fermi surfaces in URu₂Si₂ and their consequences for the HO. The existence of a FS instability had been predicted by density-functional theory (DFT) based calculations.²³ However, the importance of the occurring degenerate band-crossings in relation to the HO, and the full implications of FS nesting and the involved states have not yet been realized. Here we show that there exist two FS sheets in the paramagnetic BCT phase that are strongly nested with nesting vector $\mathbf{Q}_0=(0,0,1)$, and that the corresponding dispersions fulfill $\epsilon_1(\mathbf{k})=-\epsilon_2(\mathbf{k}\pm\mathbf{Q}_0)$. A hybridization between the two crucial uranium $5f$ states can be created by a spin-orbital fluctuation with $\Delta j_z=\pm 1$ which, as we discuss, has implications for the properties of URu₂Si₂ in the HO.

Several features of URu₂Si₂ have recently become firmly established. Quantum oscillation studies^{15,16,32} have provided a consistent picture of the extremal FS orbits. Earlier and recent inelastic neutron scattering experiments^{9,33,34} revealed two important FS nesting vectors, $\mathbf{Q}_0=(0,0,1)$, the antiferromagnetic or commensurate wavevector, and $\mathbf{Q}_1=(1\pm 0.4, 0, 0)$, the incommensurate wavevector. At these vectors, pronounced long-lived spin resonances have been detected in the HO state.¹³ First-principles DFT calculations^{23,35} have predicted a FS in good agreement with the quantum oscillation studies^{15,16,32} and also consistent with recent high-energy angle-resolved photoemission spectroscopy.³⁶ Evidently, this FS is the appropriate starting point for materials specific studies of the HO. Our focus here is on the AF commensurate nesting vector \mathbf{Q}_0 , which is half a Γ - Γ reciprocal lattice distance and is favorable for the appearance of long-range AF order at modest pressure of 0.5 GPa and AF spin excitations in the HO phase.^{23,35}

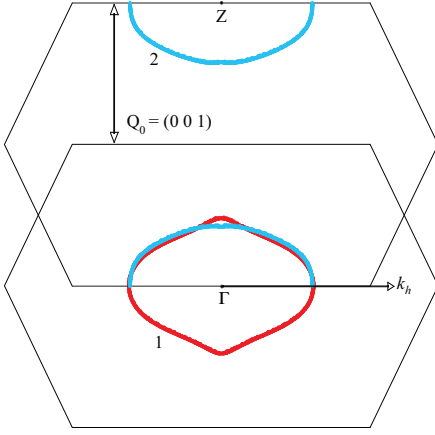


FIG. 1: (Color online) Nesting of the two essential FS sheets of URu_2Si_2 , labeled No. 1 and 2, at \mathbf{Q}_0 , illustrated for a cross-section of the BCT BZ. The cross-section has been taken through two hotspot lines, along $k_h \approx (0.5, 0.255, 0)$ and includes the $k_z = (0, 0, 1)$ axis (Γ -Z). The upper FS cross-section at Z has been shifted by \mathbf{Q}_0 to illustrate the nesting.

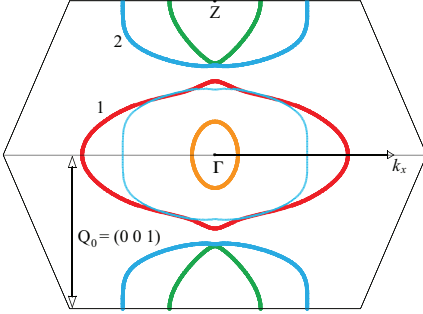


FIG. 2: (Color online) Cross-section of the BCT BZ illustrating an imperfect nesting of the two essential FS sheets No. 1 and 2 at \mathbf{Q}_0 . FS sheet No. 2 has been shifted by \mathbf{Q}_0 , and is shown by the thin light grey (color online: light blue) curve, to illustrate the imperfect nesting. The cross-section is spanned by the k_z and k_x axes. The cross-sections of two other FS pockets are shown by the green and orange lines.

Figure 1 shows the nesting of the two involved FS sheets at \mathbf{Q}_0 . The DFT calculations identified—in the BCT normal state—a Γ -centered closed FS sheet with an approximate ellipsoidal shape as well as a closed Z-centered FS sheet; these are labeled FS sheet Nos. 1 and 2. Apart from these two sheets there are three other closed FS sheets, a very small Γ -centered ellipsoid, a Z-centered ellipsoid, and an ellipsoid centered at the X point in the BCT BZ. These are not shown in Fig. 1 as they do not exhibit pronounced nesting properties. The Γ -centered sheet (dark grey, red in color online) and Z-centered sheet (light grey, blue in color online) are strongly nested with nesting vector \mathbf{Q}_0 . On these two FS sheets there are eight hotspot lines,²³ where the two FS sheets intersect when shifted by \mathbf{Q}_0 . Figure 1 illustrates the degree of nesting at a cross-section of the BZ going approximately through two FS hotspot lines as well as the Γ -Z axis. The good degree of nesting of the two FS can be recog-

nized when one overlays them (note that the lower half of FS No. 2 is shown unshifted). On the hotspot lines the nesting is in fact perfect, but since the hotspot lines are not completely straight there is a small deviation in the depicted cross-section. Also, the Γ -centered FS sheet has a pointed part close to $-Z/2$ and at $Z/2$. This “nipple” prevents a complete nesting of the two FSs.

Away from the hotspot lines the nesting is not equally good. This is illustrated in Fig. 2 where we show the FS cross-sections in another plane in the BZ, here the k_z - k_x plane. In this figure we also show two of the three other existing pockets, the Γ - and Z- centered ellipsoids. A good nesting of the two essential FS sheets 1 and 2 is present in the reciprocal space regions halfway between Γ and Z and Γ and $-Z$, again with the exception of the nipple at $Z/2$ and $-Z/2$. The nesting becomes particularly poor in the k_x direction. A similar *imperfect* nesting occurs along other planes cutting the BZ away from the hotspot lines, for example the plane spanned by k_z and the vector $(1, 1, 0)$ (not shown here).

In the energy bandstructure there are two bands which, when folded through the AF wavevector, exhibit an accidental degenerate crossing.²³ At the hotspot lines this degenerate band crossing leads to a Dirac point occurring precisely at the Fermi level,³⁵ where the band dispersions are approximately linear in the vicinity of the crossing point. Away from the hotspot lines the degenerate band crossing point falls either above (along the Γ -(1, 1, 0) direction) or below (along the Γ -(1, 0, 0) direction) the Fermi level. The relation between the energy dispersions of the two nested Fermi surfaces has not yet been given. An inspection of the bands shows that it is: $\epsilon_1(\mathbf{k}) = -\epsilon_2(\mathbf{k} \pm \mathbf{Q}_0)$. Nesting conditions of similar form, $\epsilon_1(\mathbf{k}) = -\epsilon_1(\mathbf{k} + \mathbf{Q})$, have drawn attention previously in the context of spin-density waves, orbital antiferromagnetic and spin nematic order for systems with half-filled bands.^{37,38} Recently, it was applied to URu_2Si_2 to propose spin nematic order.³¹

The orbital character of the band states of the nested FS sheets is an important aspect. As spin-orbit interaction is strong in URu_2Si_2 , spin and orbital angular momenta are not good quantum numbers; the total angular momentum j is appropriate here. All uranium 5f states in the vicinity of E_F stem from the $j=5/2$ manifold.³⁵ The j_z character of the bands near the Fermi energy is shown in Fig. 3. The relativistic band structure calculations have been performed with the Kohn-Sham-Dirac DFT formalism in the local density approximation (LDA).³⁵ The thickness of the symbols illustrates the amount of j_z spin-orbital character. This plot highlights that the U 5f-states of the Γ -centered and X-centered ellipsoids have strongly $j_z = \pm 1/2$ spin-orbital character, the Γ -centered FS No. 1 has $j_z = \pm 5/2$ character, whereas the large Z-centered FS sheet No. 2 has dominantly $j_z = \pm 3/2$ character.³⁹ The U 5f states in the two bands creating the degenerate crossing have thus distinct spin-orbital characters, differing by $\Delta j_z = \pm 1$.

The unequal spin-orbital characters of the two states

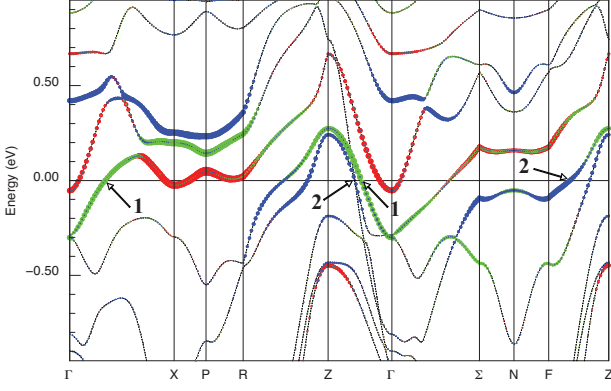


FIG. 3: (Color online) Band characters of the energy dispersions of URu_2Si_2 in the BCT BZ. Green symbols illustrate the U $5f_{5/2}$ $j_z = \pm 5/2$ character, blue symbols the $j_z = \pm 3/2$ character, and red symbols the $j_z = \pm 1/2$ character (for the used symmetry points, see Ref. 35).

has pertinent consequences for how they can interact, as these states of different symmetry cannot hybridize in the normal state, and therefore cannot lift the degeneracy. This is analogous to the Dirac crossing found in topological insulators, where the degenerate crossing of $s_z = +1/2$ and $s_z = -1/2$ bands is symmetry protected by time-reversal symmetry. In URu_2Si_2 a coupling between the two states requires a spontaneous symmetry-breaking with $\Delta j_z \neq 0$. This can be achieved by a longitudinal moment excitation with $j_z \neq 0$ which we propose to be the responsible quasiparticle acting as the coupling mediator between electrons in the two spin-orbital states. Such an AF mode at \mathbf{Q}_0 guarantees the required conservation of angular momentum j_z and linear momentum, $\mathbf{k} - \mathbf{k}' = \pm \mathbf{Q}_0$. Moment excitations with $\Delta j_z = 1$ and $\Delta j_z = -1$ are equally possible, as the nonmagnetic states in the normal phase contain equal amounts of $+j_z$ and $-j_z$ character. The required coupling of the two states over the AF vector \mathbf{Q}_0 is provided by staggered moment excitations on the U atoms in the basal plane and at the BCT vector, i.e., breaking BCT lattice symmetry.

An alternative spontaneous symmetry breaking would be a static spin density wave, that is, static AF order at \mathbf{Q}_0 , which indeed is stabilized in URu_2Si_2 at modest pressures. DFT calculations²³ predicted a very small energy difference (~ 14 K) between the normal and AF ordered states. The AF moment excitations are expected to occur at even lower energies.

The essential physics of the band hybridization can be captured in a simple model. Note that only dispersive bands are involved, not a hybridization between a localized f level and a conduction band. For the two bands only four spin-orbital $5f$ states are relevant, $j_z = \pm 3/2$ and $\pm 5/2$. Denoting the two U atoms as U_A (basal plane) and U_B (at BCT position), the degenerate states in the folded BZ ($\mathbf{k}' \pm \mathbf{Q}_0 \rightarrow \mathbf{k}$) at the band crossing can be represented as $|1\rangle_{\alpha;\pm} = |1\rangle_{\alpha,A} \pm |1\rangle_{\alpha,B}$ and $|2\rangle_{\beta;\pm} = |2\rangle_{\beta,A} \pm |2\rangle_{\beta,B}$, with $|1\rangle_{\alpha=\pm,A} = |5/2\rangle_A \pm |-5/2\rangle_A$ and

$|2\rangle_{\beta=\pm,A} = |3/2\rangle_A \pm |-3/2\rangle_A$ and analogous for atom B . A coherent spin-orbital fluctuation by $\Delta j_z = 1$ on U_A and $\Delta j_z = -1$ on U_B leads to states $|1'\rangle_{\alpha;\pm}$, $|2'\rangle_{\beta;\pm}$, for example, $|1'\rangle \propto |5/2\rangle_A + |-3/2\rangle_A + |3/2\rangle_B + |-5/2\rangle_B$ and $|2'\rangle \propto |5/2\rangle_A + |-3/2\rangle_A + |3/2\rangle_B + |-5/2\rangle_B$, allowing hybridization. A spin-orbital excitation with $\Delta j_z = -1$ on U_A and $\Delta j_z = 1$ on U_B gives the same, but with the role of U_A and U_B interchanged. The proposed quasiparticle that facilitates hybridization of the two band states is henceforth a dynamical mode of \mathbf{Q}_0 longitudinal AF excitations. Inelastic neutron scattering experiments have detected an intensive, long-lived magnetic resonance at \mathbf{Q}_0 ,^{13,33,34} which was proposed to be the dynamical driving mechanism of the HO transition.^{23,35} For completeness we mention that there exists also the incommensurate wavevector \mathbf{Q}_1 at which magnetic excitations also occur^{9,33} which alternatively have been proposed^{11,27,40} as the mechanism responsible for the HO. We find however that folding of the band dispersions at \mathbf{Q}_0 leads to a much more pronounced FS gapping.³⁵

The dynamical AF mode satisfies the $\Delta j_z = \pm 1$ condition and additionally explains other peculiar properties of URu_2Si_2 . Early inelastic neutron experiments found a magnetic longitudinal excitation with an unexpected large matrix element of $g\mu_B |j_z| \approx 1.2 - 2.2 \mu_B$,^{33,41} which is consistent with the Δj_z required for interaction of the band states. Another property of URu_2Si_2 which was not yet explained is the peculiarity that its magnetic excitations are longitudinal, i.e., Ising-like along the c -axis. In contrast, common low-energy excitations in conventional magnetic materials are transversal moment fluctuations. This unusual feature of the HO phase of URu_2Si_2 follows here from the orbital characters of the j_z -bands.

Right at the Dirac crossings there exists good particle-hole symmetry. Anomalous particle-hole pairing at bands with nesting condition $\epsilon_1(\mathbf{k}) = -\epsilon_1(\mathbf{k} + \mathbf{Q})$ – which can give rise to orbital AF or spin nematic orders^{31,37,38} – can therefore appear at the hotspot lines. However, this would be for bands with *identical* character and the situation in URu_2Si_2 is distinct. First, the unequal spin-orbital character of the involved bands should be taken into account rendering the Dirac crossing point symmetry protected. Second, the particle-hole pairing gap opened at the hotspots would be symmetric around the Fermi energy, but STS experiments detected a gap that is not symmetric around E_F .¹² Furthermore, particle-hole symmetry is not preserved at k -points not located directly on the hotspot lines. Accordingly, the particle-hole pairing gap opening at the FS would then be restricted to the immediate vicinity of the hotspot lines which implies only a modest gapping of the total FS. Experiments however find a substantial removal of about 40% of the FS in the HO.³ For URu_2Si_2 the AF excitation is a prerequisite for the hybridization. Moreover, the AF mode provides hybridization of \mathbf{Q}_0 -folded states $|1\rangle$ and $|2\rangle$ over a wide k -space region and induces a much larger FS gapping, in which degenerate crossings above and below the Fermi level become gapped, too.³⁵ Upon AF excitation

anomalous particle-hole pairing at the hotspots becomes possible which gives rise to staggered spin and charge currents^{37,38} around U atoms in the tetragonal planes. As pointed out previously³⁸ (for the situation without AF mode), such occurring static currents cause rotational symmetry breaking of the underlying tetragonal lattice and the spin currents break SU(2) spin rotational symmetry. Static staggered charge currents in the plaquette of U atoms would be detectable with neutron scattering or μ SR, but these have never been observed in URu₂Si₂.

A consequence of the dynamical spin-orbital mode is the appearance of dynamical spin and charge currents circulating around the U atoms in the plaquettes, exhibiting antiparallel rotation helicity for U atoms connected through the BCT vector. To analyze the consequences of the circulating currents we consider the two band states forming the nested FS as a minimal yet sufficient model. Circulating charge currents $j_\alpha = qp^\alpha$ around atom U_A give rise to a non-vanishing off-diagonal conductance, $\sigma_{xy} \propto iq^2 \sum_{i \neq j} (f_j - f_i) \mathcal{P} \frac{1}{(\epsilon_j - \epsilon_i)^2} p_{ij}^x p_{ji}^y$, with $i, j = |1'\rangle_A$ or $|2'\rangle_A$, q the charge, f the Fermi function, and \vec{p} the momentum operator. This gives $p_{1'2'}^x p_{2'1'}^y \neq 0$. Likewise, circulating spin currents $j_\alpha = \vec{s} p^\alpha$ lead to a non-vanishing off-diagonal spin conductance. Considering its component in the basal plane, $\propto i \sum_{i \neq j} (f_j - f_i) \mathcal{P} \frac{1}{(\epsilon_j - \epsilon_i)^2} (s^x p^x)_{ij} (s^y p^y)_{ji}$, and using that $s_{ii}^x = s_{ii}^y = 0$ (but $p_{ii}^x = \frac{m}{\hbar} \partial \epsilon_i / \partial k_x \neq 0$) one obtains $s_{1'2'}^x s_{2'1'}^y \neq 0$. As a result the off-diagonal spin susceptibility $\chi_{xy} \propto - \sum_{i \neq j} (f_j - f_i) \mathcal{P} \frac{1}{(\epsilon_j - \epsilon_i)^2} s_{ij}^x s_{ji}^y$, which contains terms $s_{1'2'}^x s_{2'1'}^y$, is nonzero. When the charge current direction reverses, σ_{xy} changes sign (as $\sigma_{yx} = -\sigma_{xy}$)

and thus the averaged off-diagonal conductance vanishes when averaged over a sufficiently long time. The averaged off-diagonal susceptibility however does not vanishes, as $\chi_{xy} = \chi_{yx}$. Hence, due to the occurrence of circulating charge and spin currents, $\chi_{xy} \neq 0$, giving a rotational symmetry breaking consistent with the nonzero susceptibility observed in recent torque measurements.²⁸

The dynamic aspect of the AF resonance is an essential difference between the HO and the long-range ordered AF phase. In the latter phase the moments are static and no oscillating currents appear in the U planes. The only breaking of the lattice symmetry is the doubling of the unit cell, giving a modulation of the c^* -axis periodicity. In the HO phase conversely the interaction of bands folded over the AF \mathbf{Q}_0 vector leads to the observed^{14,15} modulation of the lattice periodicity along the c^* -axis, and in addition the circulating currents lead to breaking of rotational symmetry in the basal planes.²⁸

To summarize, specific FS nesting conditions exist in URu₂Si₂ which are pertinent to its HO. An Ising-like excitation mode induces an interaction of two FS states connected by the \mathbf{Q}_0 vector, leading to hybridization, FS gapping, and lattice symmetry breaking in accord with recent experiments. This emphasizes that HO is a momentum space ordering phenomenon, rather than a property of a localized f configuration.

We thank S. Fujimoto for a helpful discussion. This work was supported by the Swedish Research Council (VR) and Swedish National Infrastructure for Computing (SNIC).

-
- ¹ T.T.M. Palstra, A.A. Menovsky, J. van den Berg, A.J. Dirkmaat, P.H. Kes, G.J. Nieuwenhuys, and J.A. Mydosh, Phys. Rev. Lett. **55**, 2727 (1985).
 - ² W. Schlabit, J. Baumann, B. Polit, U. Rauchschwalbe, H.M. Mayer, U. Ahlheim, and C.D. Bredl, Z. Phys. B **62**, 171 (1986).
 - ³ M.B. Maple, J.W. Chen, Y. Dalichaouch, T. Kohara, C. Rossel, M.S. Torikachvili, M.W. McElfresh, and J.D. Thompson, Phys. Rev. Lett. **56**, 185 (1986).
 - ⁴ J.A. Mydosh and P.M. Oppeneer, Rev. Modern Phys. **83** xxx (2011), arXiv:1107.0258.
 - ⁵ J. Schoenes, C. Schönenberger, J.J.M. Franse, and A.A. Menovsky, Phys. Rev. B **35**, 5375 (1987).
 - ⁶ K. Behnia, R. Bel, Y. Kasahara, Y. Nakajima, H. Jin, H. Aubin, K. Izawa, Y. Matsuda, J. Flouquet, Y. Haga, Y. Ōnuki, and P. Lejay, Phys. Rev. Lett. **94**, 156405 (2005).
 - ⁷ A. Amato, M. J. Graf, A. de Visser, H. Amitsuka, D. Andreica, and A. Schenck, J. Phys.: Condens. Matter **16**, S4403 (2004).
 - ⁸ H. Amitsuka, K. Matsuda, I. Kawasaki, K. Tenya, M. Yokoyama, C. Sekine, N. Tateiwa, T.C. Kobayashi, S. Kawarazaki, and H. Yoshizawa, J. Magn. Magn. Mater. **310**, 214 (2007).
 - ⁹ C.R. Wiebe, J.A. Janik, G.J. Macdougall, G.M. Luke, J.D. Garrett, H.D. Zhou, Y.J. Yo, L. Balicas, Y. Qiu, J.R.D. Copley, Z. Yamani, and W.J.L. Buyers, Nature Phys. **3**, 96 (2007).
 - ¹⁰ A.F. Santander-Syro, M. Klein, F.L. Boariu, A. Nuber, P. Lejay, and F. Reinert, Nature Phys. **5**, 637 (2009).
 - ¹¹ A.R. Schmidt, M.H. Hamidian, P. Wahl, F. Meier, A.V. Balatsky, J.D. Garrett, T.J. Williams, G.M. Luke, and J.C. Davis, Nature (London) **465**, 570 (2010).
 - ¹² P. Aynajian, E.H. da Silva Neto, C.V. Parker, Y. Huang, A. Pasupathy, J.A. Mydosh, and A. Yazdani, Proc. Natl. Acad. USA **107**, 10383 (2010).
 - ¹³ F. Bourdarot, E. Hassinger, S. Raymond, D. Aoki, V. Taufour, L.-P. Regnault, and J. Flouquet, J. Phys. Soc. Jpn. **79**, 064719 (2010).
 - ¹⁴ R. Yoshida, Y. Nakamura, M. Fukui, Y. Haga, E. Yamamoto, Y. Ōnuki, M. Okawa, S. Shin, M. Hirai, Y. Muraoka, and T. Yokoya, Phys. Rev. B **82**, 205108 (2010).
 - ¹⁵ E. Hassinger, G. Knebel, T. D. Matsuda, D. Aoki, V. Taufour, and J. Flouquet, Phys. Rev. Lett. **105**, 216409 (2010).
 - ¹⁶ M.M. Altarawneh, N. Harrison, S.E. Sebastian, L. Balicas, P.H. Tobash, J.D. Thompson, F. Ronning, and E.D. Bauer, Phys. Rev. Lett. **106**, 146403 (2011).
 - ¹⁷ G.L. Dakovski *et al.*, ArXiv:cond-mat/1104.3869.
 - ¹⁸ P. Santini and G. Amoretti, Phys. Rev. Lett. **73**, 1027 (1994).
 - ¹⁹ H. Ikeda and Y. Ohashi, Phys. Rev. Lett. **81**, 3723 (1998).

- ²⁰ P. Chandra, P. Coleman, J.A. Mydosh, and V. Tripathi, *Nature* **417**, 831 (2002).
- ²¹ V.P. Mineev and M.E. Zhitomirsky, *Phys. Rev. B* **72**, 014432 (2005).
- ²² C.M. Varma and L. Zhu, *Phys. Rev. Lett.* **96**, 036405 (2006).
- ²³ S. Elgazzar, J. Rusz, M. Amft, P.M. Oppeneer, and J.A. Mydosh, *Nature Mater.* **8**, 337 (2009).
- ²⁴ K. Haule and G. Kotliar, *Nature Phys.* **5**, 796 (2009).
- ²⁵ F. Cricchio, F. Bultmark, O. Grånäs, and L. Nordström, *Phys. Rev. Lett.* **103**, 107202 (2009).
- ²⁶ H. Harima, K. Miyake, and J. Flouquet, *J. Phys. Soc. Jpn.* **79**, 033705 (2010).
- ²⁷ Y. Dubi and A.V. Balatsky, *Phys. Rev. Lett.* **106**, 086401 (2011).
- ²⁸ R. Okazaki, T. Shibauchi, H. J. Shi, Y. Haga, T. D. Matsuda, E. Yamamoto, Y. Onuki, H. Ikeda, and Y. Matsuda, *Science* **331**, 439 (2011).
- ²⁹ P. Thalmeier and T. Takimoto, *Phys. Rev. B* **83**, 165110 (2011).
- ³⁰ C. Pépin, M.R. Norman, S. Burdin, and A. Ferraz, *Phys. Rev. Lett.* **106**, 106601 (2011).
- ³¹ S. Fujimoto, *Phys. Rev. Lett.* **106**, 196407 (2011).
- ³² H. Ohkuni, Y. Inada, Y. Tokiwa, K. Sakurai, R. Settai, T. Honma, Y. Haga, E. Yamamoto, Y. Ōnuki, H. Yamagami, S. Takahashi, and T. Yanagisawa, *Phil. Mag. B* **79**, 1045 (1999).
- ³³ C. Broholm, H. Lin, P.T. Matthews, T.E. Mason, W.J.L. Buyers, M.F. Collins, A.A. Menovsky, J.A. Mydosh, and J.K. Kjems, *Phys. Rev. B* **43**, 12809 (1991).
- ³⁴ A. Villaume, F. Bourdarot, E. Hassinger, S. Raymond, V. Taufour, D. Aoki, and J. Flouquet, *Phys. Rev. B* **78**, 012504 (2008).
- ³⁵ P.M. Oppeneer, J. Rusz, S. Elgazzar, T. Durakiewicz, and J.A. Mydosh, *Phys. Rev. B* **82**, 205103 (2010).
- ³⁶ I. Kawasaki, S.-i. Fujimori, Y. Takeda, T. Okane, A. Yasui, Y. Saitoh, H. Yamagami, Y. Haga, E. Yamamoto, and Y. Ōnuki, *Phys. Rev. B* **83**, 235121 (2011).
- ³⁷ H.J. Schulz, *Phys. Rev. B* **39**, 2940 (1989).
- ³⁸ A.A. Nersisyan, G.I. Japaridze, and I.G. Kimeridze, *J. Phys.: Cond. Matter* **3**, 3353 (1991).
- ³⁹ Note that the j_z character changes in the poorly nested lobes of FS No. 1, which do not participate in the gapping.
- ⁴⁰ A.V. Balatsky, A. Chantis, H.P. Dahal, D. Parker, and J.X. Zhu, *Phys. Rev. B* **96**, 214413 (2009).
- ⁴¹ C. Broholm, J.K. Kjems, W.J.L. Buyers, P. Matthews, T.T.M. Palstra, A.A. Menovsky, and J.A. Mydosh, *Phys. Rev. Lett.* **58**, 1467 (1987).